

Submitted to  
*Nucl. Phys. B*

MPI-PhT/97-20  
BUTP-97/08  
gr-qc/9703047  
March 18, 1997

# Mass inflation and chaotic behaviour inside hairy black holes

Peter Breitenlohner <sup>†</sup>, George Lavrelashvili <sup>‡</sup> <sup>1</sup>  
and Dieter Maison <sup>†</sup>

*Max-Planck-Institut für Physik* <sup>†</sup>  
— *Werner Heisenberg Institut* —  
*Föhringer Ring 6*  
80805 Munich (Fed. Rep. Germany)

*Institute for Theoretical Physics* <sup>‡</sup>  
*University of Bern*  
*Sidlerstrasse 5*  
*CH-3012 Bern, Switzerland*

## Abstract

We analyze the interior geometry of static, spherically symmetric black holes of the Einstein-Yang-Mills-Higgs theory. Generically the solutions exhibit a behaviour that may be described as “mass inflation”, although with a remarkable difference between the cases with and without a Higgs field. Without Higgs field the YM field induces a kind of cyclic behaviour leading to repeated cycles of mass inflation – taking the form of violent explosions – interrupted by quiescent periods and subsequent approaches to an almost Cauchy horizon. With the Higgs field no such cycles occur. In addition there are non-generic families with a Schwarzschild resp. Reissner-Nordström type singularity at  $r = 0$ .

---

<sup>1</sup>On leave of absence from Tbilisi Mathematical Institute, 380093 Tbilisi, Georgia

# 1 Introduction

Most of the knowledge on the interior geometry of static black holes derives from the well-known exact solutions like the Schwarzschild (S) and Reissner-Nordström (RN) solution. Whereas for the S-solution the radial coordinate stays time-like inside the horizon all the way down to the central singularity, the RN-solution exhibits a second – inner – horizon, behind which the radial coordinate becomes space-like again. This inner horizon is a so-called Cauchy horizon, beyond which the evolution of any matter system is influenced by data causally disconnected from the earlier history [1]. Furthermore, while the outer horizon is an infinite redshift surface, the Cauchy horizon is a surface of infinite blueshift. This suggests, that the Cauchy horizon should be unstable against small perturbations and a space-like singularity should form replacing the former Cauchy horizon [2]. In fact, perturbative studies indicate an exponential growth of the mass-function close to the inner horizon – a phenomenon dubbed “mass inflation” [2]. However, as yet no unanimous conclusion about the reliability and genericity of these perturbative results seems to have been obtained [3]. In this situation it is definitely of interest to investigate the internal structure of black holes with other forms of matter like Yang-Mills and Higgs fields. This is the subject of the present study. Compared to the previously mentioned perturbative analysis our work is “exact”, although at least partially based on numerical results.

One may summarize these results saying that generically no Cauchy horizon forms, because its existence requires fine-tuning of the initial data at the outer horizon. Solutions with a Cauchy horizon are in fact obtained through such fine-tuning, leading to a RN-type singularity at  $r = 0$ . Generically, however, the solutions exhibit “mass-inflation”, although with a remarkable difference between the cases with and without a Higgs field. The behaviour is actually much simpler with the inclusion of a Higgs field. In this case the mass function shows generically exponential growth all the way down to  $r = 0$ . On the other hand in the seemingly simpler case without the Higgs field the situation is more involved. The YM field induces a kind of cyclic behaviour leading to repeated cycles of mass inflation – taking the form of violent “explosions” – interrupted by quiescent periods and subsequent approaches to an almost Cauchy horizon. This behaviour is particularly spectacular due to the fantastic growth of the mass function during these explosions by hundreds of orders of magnitude, a phenomenon unprecedented in standard physical

problems. Actually, these explosions become exponentially more violent after each cycle such that it is practically impossible to follow more than one or two of them numerically.

A further novel phenomenon is a kind of chaotic behaviour generated by a hierarchical structure of families of non-abelian RN-type (NARN) and non-abelian S-type (NAS) solutions separating generic solutions with cyclic (EYM) or acyclic (EYMH) behaviour.

Our numerical results exhibiting these claims are predominately based on the EYM system, but we have no doubt that we could easily establish similarly convincing evidence in the EYMH case.

In this discussion the global behaviour outside the horizon was ignored. Clearly it is of interest to find out what is the behaviour of asymptotically flat solutions, which for the EYM theory constitute a discrete set of 1-parameter families – described by curves in the  $(W_h, r_h)$  plane [4, 5]. Obviously without further restriction they will show the generic behaviour inside the horizon, although for certain discrete points S-type resp. RN-type singularities at  $r = 0$  are possible.

In a recent paper [6] Donets et al. presented their results on the internal structure of static, spherically symmetric black holes of the Einstein-Yang-Mills (EYM) theory (without Higgs field). Our results for this particular case essentially agree with the findings of Donets et al., although we differ in some details. In particular the chaotic structure we find close to the basic NARN solutions was not observed in [6].

## 2 Ansatz and Field Equations

The contents of this chapter are essentially (up to minor changes in notation) a copy from our earlier paper [7], which we include for the convenience of the reader.

For the static, spherically symmetric metric we use the parametrization

$$ds^2 = A^2 B dt^2 - \frac{dR^2}{B} - r^2(R) d\Omega^2, \quad (1)$$

with  $d\Omega^2 = d\theta^2 + \sin^2 \theta d\varphi^2$  and three independent functions  $A$ ,  $B$ ,  $r$  of a radial coordinate  $R$ , which has, in contrast to  $r$ , no geometrical significance.

It is common to express  $B$  through the “mass function”  $m$  defined by  $B = 1 - 2m/r$ .

For the  $SU(2)$  Yang-Mills field  $W_\mu^a$  we use the standard minimal spherically symmetric (purely ‘magnetic’) ansatz

$$W_\mu^a T_a dx^\mu = W(R)(T_1 d\theta + T_2 \sin \theta d\varphi) + T_3 \cos \theta d\varphi, \quad (2)$$

and for the Higgs field we assume the form

$$\Phi^a T_a = H(R) n^a T_a, \quad (3)$$

where  $T_a$  denote the generators of  $SU(2)$  in the adjoint representation. Plugging these ansätze into the EYMH action results in

$$S = - \int dRA \left[ \frac{1}{2} \left( 1 + B((r')^2 + \frac{(A^2 B)'}{2A^2 B} (r^2)') \right) - Br^2 V_1 - V_2 \right], \quad (4)$$

with

$$V_1 = \frac{(W')^2}{r^2} + \frac{1}{2} (H')^2, \quad (5)$$

and

$$V_2 = \frac{(1 - W^2)^2}{2r^2} + \frac{\beta^2 r^2}{8} (H^2 - \alpha^2)^2 + W^2 H^2. \quad (6)$$

Through a suitable rescaling we have achieved that the action depends only on the dimensionless parameters  $\alpha$  and  $\beta$  representing the mass ratios  $\alpha = M_W \sqrt{G}/g = M_W/gM_{\text{Pl}}$  and  $\beta = M_H/M_W$  ( $g$  denoting the gauge coupling and  $G$  Newtons constant).<sup>2</sup>

We still have to choose a suitable gauge for the radial coordinate  $R$ . The most natural choice is  $R \equiv r$ , i.e. Schwarzschild (S) coordinates. However, this choice is singular at a stationary point of  $r(R)$  (‘equator’). Such singularities are avoided using the gauge  $B \equiv r^{-2}$  for  $B > 0$  resp.  $B \equiv -r^{-2}$  for  $B < 0$ . We denote this radial coordinate by  $\tau$  in order to distinguish it from the S coordinate  $r$ . With this choice the spatial part of the metric takes the simple form

$$ds^2 = r^2(d\tau^2 + d\Omega^2), \quad (7)$$

---

<sup>2</sup> The usual quantum definition of  $M_{\text{Pl}} \equiv \sqrt{\frac{\hbar c}{G}}$  is obtained from our classical expression replacing the dimensionful classical gauge coupling  $g^2$  by the dimensionless  $\frac{g^2}{\hbar c}$  and putting the latter equal to one.

suggesting to call them isotropic coordinates.

Using S coordinates the field equations obtained from (4) are

$$(BW')' = W\left(\frac{W^2 - 1}{r^2} + H^2\right) - 2rBW'V_1, \quad (8a)$$

$$(r^2BH')' = (2W^2 + \frac{\beta^2 r^2}{2}(H^2 - \alpha^2))H - 2r^3BH'V_1, \quad (8b)$$

$$(rB)' = 1 - 2r^2BV_1 - 2V_2, \quad (8c)$$

$$A' = 2rV_1A. \quad (8d)$$

The equations obtained with isotropic coordinates  $B \equiv -r^{-2}$  are essentially Eqs. (9) of [7], there are however some sign changes due to  $B < 0$ .

$$r' = rN, \quad (9a)$$

$$N' = (\kappa - N)N - 2U^2 - V^2, \quad (9b)$$

$$\kappa' = -1 - \kappa^2 + 2U^2 + \frac{\beta^2 r^2}{2}(H^2 - \alpha^2)^2 + 2H^2W^2, \quad (9c)$$

$$W' = rU, \quad (9d)$$

$$U' = -\frac{W(W^2 - 1)}{r} - rH^2W - (\kappa - N)U, \quad (9e)$$

$$H' = V, \quad (9f)$$

$$V' = -\frac{\beta^2 r^2}{2}(H^2 - \alpha^2)H - 2W^2H - \kappa V, \quad (9g)$$

together with the constraint

$$2\kappa N = -1 + N^2 + 2U^2 + V^2 + 2V_2, \quad (10)$$

and the definitions

$$N \equiv \frac{r'}{r}, \quad \kappa \equiv \frac{(A^2B)'}{2A^2B} + N, \quad U \equiv \frac{W'}{r}, \quad \text{and} \quad V \equiv H'. \quad (11)$$

### 3 Singular points

The field Eqs. (8) are singular at  $r = 0$ ,  $r = \infty$  and for points where  $B$  vanishes. Whereas the former singularities are of geometrical origin (the action of the rotation group degenerates) the zeros of  $B$  turn out to be coordinate singularities, in fact, of two different kinds:

1. Points where  $B = 0$ , but  $A^2B \neq 0$  are stationary points of the function  $r(R)$  and hence choosing  $r$  as a coordinate leads to singular derivatives; our second coordinate choice avoids this problem.
2. Points where  $B = 0$  and  $A^2 < \infty$  correspond to an horizon; as is well known a retarded time coordinate  $t^* = t - \int \frac{dr}{A|B|}$  avoids this singularity.

As we want to stick to the time coordinate  $t$  we have to treat horizons as singular points. In order to guarantee the finiteness of  $A$  we have to require the regularity conditions

$$rB'|_h = 1 - 2V_2|_h, \quad B'W'|_h = \frac{1}{2} \frac{\partial V_2}{\partial W} \Big|_h, \quad r^2B'H'|_h = \frac{\partial V_2}{\partial H} \Big|_h. \quad (12)$$

In general it is not possible to parametrize regular solutions directly by their initial data at the singular point. However, as was already discussed in [5, 8, 7] in the present case this is in fact possible, using a sharpened version (Prop. 1 of [5]) of the standard text-book existence theorems [9].

*Proposition:*

Consider a system of first order differential Eqs. for  $m+n$  functions  $y = (u, v)$

$$s \frac{du_i}{ds} = s f_i(s, y), \quad i = 1, \dots, m, \quad (13a)$$

$$s \frac{dv_i}{ds} = -\lambda_i v_i + s g_i(s, y), \quad i = 1, \dots, n, \quad (13b)$$

with constants  $\lambda_i > 0$  and let  $\mathcal{C}$  be an open subset of  $\mathbf{R}^m$  such that  $f_i, g_i$  are analytic in a neighbourhood of  $s = 0, y = (c, 0)$  for all  $c \in \mathcal{C}$ . There exists an  $m$ -parameter family of local solutions  $y_c(s)$  analytic in  $c$  and  $s$  for  $c \in \mathcal{C}, |s| < s_0(c)$  such that  $y_c(0) = (c, 0)$ .

In order to meet the requirements of this Proposition we may introduce the coordinate  $s \equiv r - r_h$  and put [8]

$$u_1 \equiv r, \quad u_2 \equiv W, \quad u_3 \equiv H, \quad (14a)$$

$$v_1 \equiv \frac{B}{s} - \frac{1}{u_1} \left( 1 - 2V_2 \right), \quad (14b)$$

$$v_2 \equiv \frac{BW'}{s} - u_2 \left( \frac{u_2^2 - 1}{u_1^2} + u_3^2 \right), \quad (14c)$$

$$v_3 \equiv \frac{r^2 B H'}{s} - u_3 \left( 2u_2^2 + \frac{\beta^2}{2} u_1^2 (u_3^2 - 1) \right). \quad (14d)$$

There remain two parameters –  $W_h$  and  $H_h$  – to describe solutions with a regular horizon at  $r_h$ . For an event horizon  $r$  has to increase as one deviates from the horizon in the direction where  $B$  is positive. This requires the inequality

$$rB'|_h = 1 - 2V_2|_h > 0 , \quad (15)$$

which for the case without Higgs field reduces to  $r_h > |W_h^2 - 1|$ . For  $V_2|_h = 1/2$  we get  $B'|_h = 0$ , which looks like the condition for a degenerate horizon. As discussed in [7] the latter is, however, only obtained for  $1 - 2V_2|_h = \partial V_2/\partial W|_h = \partial V_2/\partial H|_h = 0$ ; without Higgs field this is satisfied only for  $r_h = 1$ ,  $W_h = 0$  yielding the extremal Reissner-Nordström solution. Initial data with  $V_2|_h = 1/2$  but  $\partial V_2/\partial W|_h \neq 0$  and/or  $\partial V_2/\partial H|_h \neq 0$  turn out to describe a non-degenerate horizon, which is simultaneously a maximum of  $r$  and therefore has a singularity in S coordinates. In order to avoid this singular behavior one may use isotropic coordinates, in which the boundary conditions at the horizon (assumed to be at  $\tau = 0$ ) read [7]

$$r(\tau) = r_h \left( 1 + N_1 \left( \frac{\tau^2}{2} + O(\tau^4) \right) - \left( W_1^2 + \frac{1}{2} H_1^2 \right) \frac{\tau^4}{4} \right) + O(\tau^6) , \quad (16a)$$

$$N(\tau) = N_1(\tau + O(\tau^3)) - \left( W_1^2 + \frac{1}{2} H_1^2 \right) \tau^3 + O(\tau^5) , \quad (16b)$$

$$W(\tau) = W_h + r_h W_1 \frac{\tau^2}{2} + O(\tau^4) , \quad (16c)$$

$$H(\tau) = H_h + H_1 \frac{\tau^2}{2} + O(\tau^4) , \quad (16d)$$

where

$$N_1 = -\frac{1}{2} + V_2|_h , \quad W_1 = -\frac{r_h}{4} \frac{\partial V_2}{\partial W} \Big|_h , \quad H_1 = -\frac{1}{2} \frac{\partial V_2}{\partial H} \Big|_h , \quad (17)$$

The function  $\kappa(\tau)$  has a simple pole at the horizon, but  $\kappa(\tau) - 1/\tau$  is regular.  $B \equiv -N^2$ ,  $W$ , and  $H$  are analytic in  $\tau^2$  and  $\tau^2$  is analytic in the S coordinate  $r$  as long as  $V_2|_h \neq 1/2$  (i.e.,  $N_1 \neq 0$ ). For the special case  $V_2|_h = 1/2$  we obtain

$$B = -8(W_1^2 + H_1^2/2)^{\frac{1}{2}}(1 - r/r_h)^{\frac{3}{2}} + O((1 - r/r_h)^2) , \quad (18a)$$

$$W = W_h + r_h W_1 \left( \frac{1 - r/r_h}{W_1^2 + H_1^2/2} \right)^{\frac{1}{2}} + O(1 - r/r_h) , \quad (18b)$$

$$H = H_h + H_1 \left( \frac{1 - r/r_h}{W_1^2 + H_1^2/2} \right)^{\frac{1}{2}} + O(1 - r/r_h) . \quad (18c)$$

In the following we will use the terms event resp. Cauchy horizon for any horizon with  $B'|_h > 0$  resp.  $< 0$ , although the original meaning of these terms applies only to asymptotically flat solutions.

Next we turn to the singular behaviour at  $r = 0$ , which is of particular relevance for the internal structure of black hole solutions. We have to distinguish two cases,  $B > 0$  and  $B < 0$ .

1.  $B > 0$ : For black holes this case is only possible, if there is a second, inner horizon. The generic behaviour of the solutions in isotropic coordinates without the Higgs field is described by Prop. 13 of [5]. Translating to S coordinates and taking into account the Higgs field we get

$$W(r) = W_0 + \frac{W_0}{2(1 - W_0^2)} r^2 + W_3 r^3 + O(r^4) , \quad (19a)$$

$$H(r) = H_0 + H_1 r + O(r^2) , \quad (19b)$$

$$B(r) = \frac{(W_0^2 - 1)^2}{r^2} - \frac{2M_0}{r} + O(1) , \quad (19c)$$

which is a 5-parameter, i.e. generic, family of solutions. In the case with vanishing Higgs field Prop. 13 of [5] implies the analyticity of  $W(r)$  and  $r^2 B(r)$ , i.e. the expressions above are in fact the beginning of a convergent Taylor series. More generally, in the case with a Higgs field, introducing the variables

$$u_1 \equiv W , \quad u_2 \equiv (rBW' + W(W^2 - 1))/r , \quad (20a)$$

$$u_3 \equiv \left( \frac{(W^2 - 1)^2}{r^2 B} - 1 \right) / r , \quad (20b)$$

$$u_4 \equiv H , \quad u_5 \equiv H' , \quad (20c)$$

it is easy so check that

$$ru'_i = O(r) , \quad i = 1 \dots 5 , \quad (21)$$

and thus analyticity follows from the Proposition with  $\mathcal{C} = \{W_0^2 \neq 1\}$ .



According to the asymptotics of  $B(r)$  we may call the singular behaviour to be of RN-type. The special case  $W_0^2 = 1, M_0 < 0$  leads to S-type behavior with a naked singularity. On the other hand  $W_0^2 = 1, H_0 = 0, M_0 = 0$  gives regular solutions.

2.  $B < 0$ : This case is more involved, with two disjoint families of singular solutions.
- 2.1 There is a 3-parameter family of solutions with a S-type singularity, characterized by the asymptotics

$$W(r) = 1 + W_2 r^2 + O(r^3) , \quad (22a)$$

$$H(r) = H_0 + O(r) , \quad (22b)$$

$$B(r) = -\frac{2M_0}{r} + O(1) . \quad (22c)$$

Introducing the variables

$$u_1 \equiv BW' , \quad u_2 \equiv \frac{1}{rB} , \quad u_3 \equiv H , \quad (23a)$$

$$v_1 \equiv \frac{(1 - W^2)}{r^2} + \frac{W'}{2r} , \quad (23b)$$

$$v_2 \equiv rBH' - 2H , \quad (23c)$$

we obtain

$$ru'_i = O(r) , \quad \text{for } i = 1 \dots 3 , \quad (24a)$$

$$rv'_1 = -2v_1 + O(r) , \quad rv'_2 = -v_2 + O(r) . \quad (24b)$$

With  $\mathcal{C} = \{M_0 > 0\}$  the analyticity follows again from the Proposition. Obviously the condition  $B < 0$  ( $M_0 > 0$ ) prevents the existence of regular solutions in this case.

- 2.2 There is an additional 2-parameter family of solutions with a pseudo-RN singularity (pseudo because  $B < 0$ ).

$$W(r) = W_0 \pm r + O(r^2) , \quad (25a)$$

$$H(r) = H_0 + O(r^2) , \quad (25b)$$

$$B(r) = -\frac{(W_0^2 - 1)^2}{r^2} \pm \frac{4W_0(1 - W_0^2)}{r} + O(1) . \quad (25c)$$

Introducing the variables

$$u_1 \equiv W, \quad u_2 \equiv H, \quad (26a)$$

$$v_1 \equiv \left[ 1 \mp \left( W' - \frac{W(W^2 - 1)}{rB} \right) \right] / r, \quad v_3 \equiv H', \quad (26b)$$

$$v_2 \equiv \left( \frac{(W^2 - 1)^2}{r^2 B} + 1 \right) / r, \quad (26c)$$

we get

$$ru'_i = O(r) \quad \text{for } i = 1, 2 \quad (27a)$$

$$rv'_1 = -2v_1 - 4v_2 + O(r), \quad rv'_2 = v_1 - v_2 + O(r), \quad (27b)$$

$$rv'_3 = -v_3 + O(r). \quad (27c)$$

With  $\mathcal{C} = \{W_0^2 \neq 1\}$  the Proposition implies again analyticity. The negative eigenvalues of the linearized equations are  $\lambda_{1,2} = -1/2(3 \pm i\sqrt{15})$  and  $\lambda_3 = -1$ . This is a repulsive focal point which will turn out to be important for the cyclic behaviour in the EYM case.

In the case  $B < 0$  we obtained no singular class that has enough parameters (three for EYM and five for EYMH) to describe the generic behaviour. Since, also the appearance of a second, inner horizon is a non-generic phenomenon, one may wonder, what the generic behaviour inside the horizon near  $r = 0$  looks like. This question actually is at the origin of our interest in this problem. Some insight was obtained by a detailed numerical study, whose results will be presented in the next chapter (compare also [6]).

Finally we would like to address the question of geodesic incompleteness inside the horizon expected in view of general singularity theorems [1]. We will show that for solutions without a Cauchy horizon (i.e.,  $B < 0$  for  $r < r_h$ ) the radial time- and lightlike geodesics are incomplete. Their equations are

$$g_{tt} \left( \frac{dt}{d\tau} \right)^2 - g_{rr} \left( \frac{dr}{d\tau} \right)^2 = \epsilon \quad \text{with } \epsilon = 1 \text{ or } 0. \quad (28)$$

From staticity we get the constancy of  $g_{tt} dt/d\tau = E$  and thus

$$\left( \frac{dr}{d\tau} \right)^2 = \frac{E^2}{A^2} - \epsilon B. \quad (29)$$

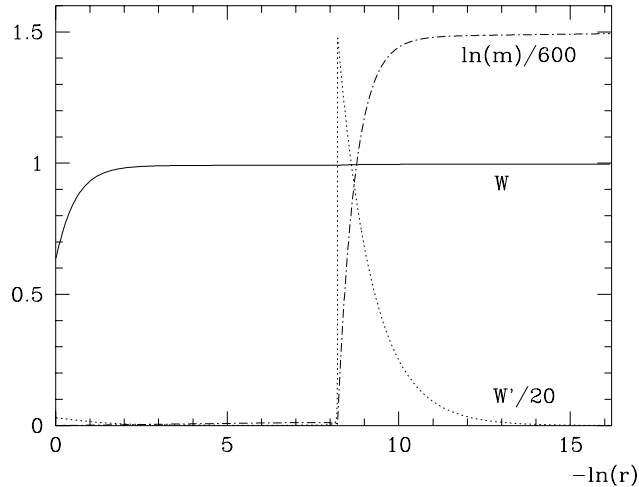


Figure 1: First inflationary cycle of the fundamental black hole of EYM theory with  $r_h = 1$  and  $W_h = 0.6322$ .

From Eq. (8d) we see that  $A$  is a monotone function of  $r$  implying

$$\tau_h \leq \int_0^{r_h} \frac{A}{E} dr \leq \frac{A(r_h)}{E} r_h < \infty, \quad (30)$$

where  $\tau_h$  is the difference in proper time resp. affine parameter between the horizon and the origin.

## 4 Numerical results

In order to investigate the generic behaviour of non-abelian black holes inside the event horizon, we integrate the field Eqs. (8) resp. (9) from the horizon assuming  $B < 0$ , ignoring the constraints on the initial data at the horizon required for asymptotic flatness.

As mentioned before, the horizon is a singular point of the equations. Consequently one has to desingularize the equations in order to be able to start the integration right there. How this can be done, was described in the previous chapter resp. in [7, 8].

If one ignores the behaviour of the solutions outside the horizon, one may relax the condition (15) ensuring a decreasing resp. increasing  $r$  inside resp. outside the horizon. At least part of the solutions violating (15) possess an equator, i.e. a maximum of  $r$ . For those the use of S coordinates is excluded.

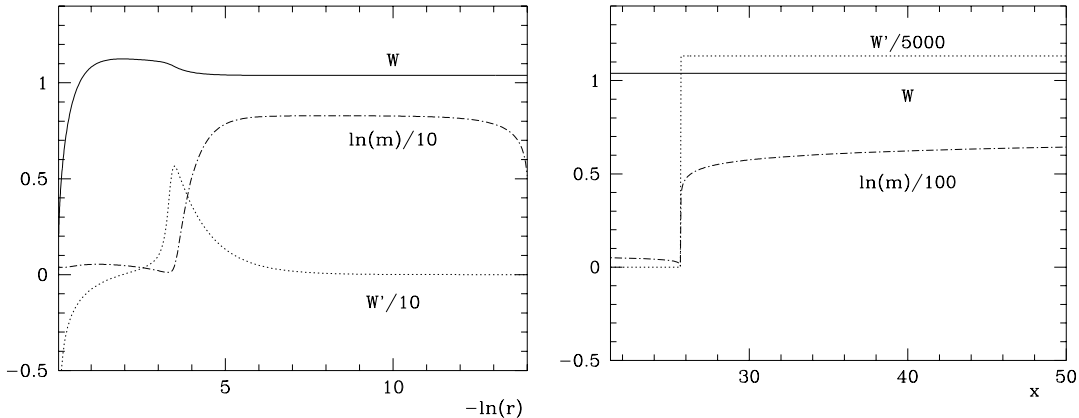


Figure 2: First two cycles of the solution with  $r_h=0.97$  and  $W_h = 0.2$ . For the second cycle a suitably stretched coordinate  $x$  is used.

As one performs the numerical integration one quickly runs into serious problems due to the occurrence of a quasi-singularity, initiated by a sudden step raise of  $W'$  and subsequent exponential growth of  $B$  resp.  $m$  (compare Figs. 1, 2, and 3 for some examples). This inflationary behaviour of the mass function is similar to the one observed for perturbations of the RN solution at the Cauchy horizon [2]. While this exponential growth continues indefinitely for the EYMH system, it comes to a stop without the Higgs field. The mass function reaches a plateau and stays constant for a while until it starts to decrease again. When  $B$  has become small enough, i.e. the solution comes close to an inner horizon, the same inflationary process repeats itself. Generically this second “explosion” is so violent (we will give estimates on the increase of  $m$  in chapter 5) that the numerical integration procedure breaks down.

Besides these generic solutions there are certain families of special solutions obtained through suitable fine-tuning of the initial data at the horizon. There are two classes of such special solutions. The first class are black holes with a second, inner horizon, the second are solutions with one of the singular behaviours at  $r = 0$  for  $B < 0$  described in chapter 3. The numerical construction of such solutions is complicated by the fact that both boundary points are singular points of the equations. The strategies employed to solve such problems are well described in our paper on gravitating monopoles [7]. Actually, in order to control the numerical uncertainties we used two differ-

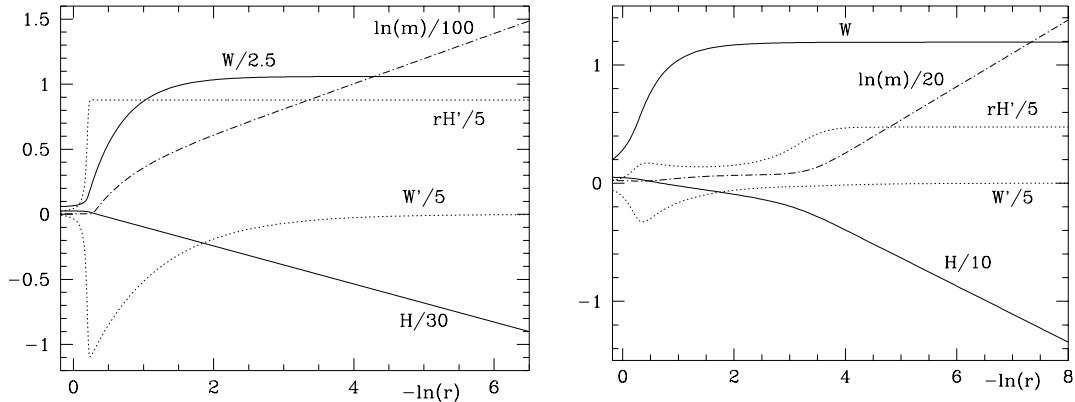


Figure 3: Inflationary solutions with Higgs fields with  $\alpha = 0.2$ ,  $\beta = 0$ ,  $r_h = 1.2$  and  $W_h = 0.15$ ,  $H_h = 0.8$  resp.  $W_h = 0.2$ ,  $H_h = 0.5$ .

ent methods, which may be called “matching” and “shooting and aiming”. For matching we integrate independently from both boundary points with regular initial data, tuning these data at both ends until the two branches of the solution match. For shooting and aiming we integrate only from one end and try to suppress the singular part of the solution at the other end by suitably tuning the initial data at the starting point.

As already said, the first class of special solutions consists of black holes with a second, inner horizon; let us call them non-abelian RN-type (NARN) solutions. As was explained in chapter 3 a regular horizon requires the simultaneous vanishing of  $B$ ,  $BW'$  and  $BH'$ . We have determined two such 1-parameter families for the EYM system, shown in Fig. 4, whose significance will be explained in chapter 5. As may be inferred from Fig. 4, the (dotted) curve 2 corresponding to one such family intersects all (solid) curves describing asymptotically flat solutions except the one for  $n = 1$ . In contrast to what is claimed by Donets et al. [6] our curve continues straight through the parabola  $r_h = 1 - W_h^2$  and runs all the way to  $r_h = W_h = 0$ . As already mentioned the branch to the left of the parabola cannot be obtained using S coordinates. The corresponding curve of Donets et al. makes a suspiciously sharp turn very close to the parabola and runs to the point  $r_h = 1, W_h = 0$ . We are convinced that the latter piece of their curve is an artefact of unreliable numerics caused by the use of S coordinates becoming singular at the parabola (compare the discussion in chapter 3).

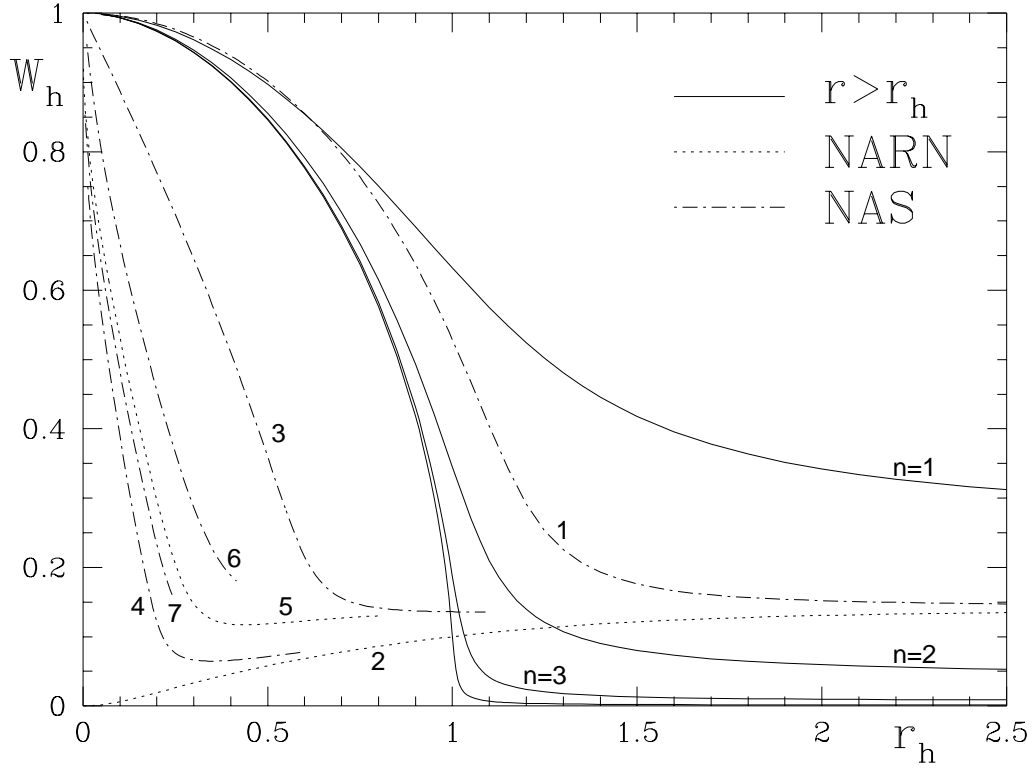


Figure 4: Initial data for special solutions. The solid curves represent asymptotically flat solutions with  $n$  zeros of  $W$ . The other curves represent various NARN and NAS families.

As already stressed  $B'$  has to be positive at an event horizon. This condition is violated for values of  $r_h < r_p$ , where  $r_p$  denotes the value of  $r_h$  where the NARN curve 2 intersects the parabola. However it turns out to be fulfilled for the second horizon if  $r_h < r_m$  with  $r_m \approx 0.112$  on the NARN curve. Thus this curve may be divided into three pieces according to  $0 < r_h < r_m$ ,  $r_m < r_h < r_p$  and  $r_p < r_h$ . On the first interval the two horizons have exchanged their roles, whereas on the second interval both of them are Cauchy horizons with a maximum of  $r$  (equator) in between. The only difference between the first and the third interval is that  $W_h > 1$  resp.  $< 1$  on the event horizon.

Our second NARN family (curve 5 of Fig. 4) stays completely to the left of the parabola and ends at  $r_h \approx 0.9$  close to the curve 3, whose significance

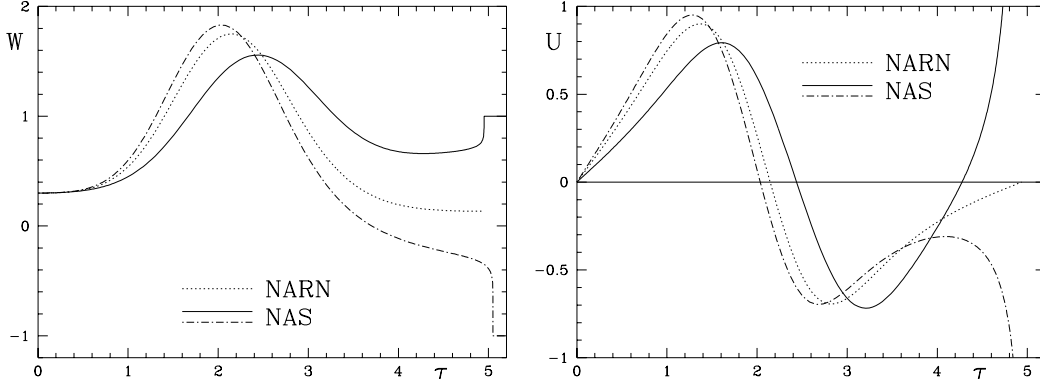


Figure 5: A NARN solution and two accompanying NAS solutions with  $W_h = 0.3$  and  $r_h = 0.198728$  (on curve 5 of Fig. 4),  $r_h = 0.290837$  (on curve 6 with  $W \rightarrow +1$ ), and  $r_h = 0.170525$  (on curve 7 with  $W \rightarrow -1$ ).

will be explained below.

The second class are solutions without a second horizon (i.e.  $B$  stays negative) approaching the center  $r = 0$  with one of the two singular behaviours described in chapter 3, i.e. those with a S-type singularity resp. with a pseudo-RN-type singularity; let us denote them NAS resp. NAPRN solutions. We have determined several NAS families represented by the dashed-dotted curves of Fig. 4. The curve 1 staying to the right of the parabola coincides with the corresponding one of Donets et al., whereas the others, staying essentially to the left of the parabola are new. As will be explained in chapter 5, the two NAS curves 6 and 7 accompanying the (dotted) NARN curve 5 are expected to merge with the NAS curve 3 close to  $r_h = 0.9$ . Some of the NAS curves (e.g., 3 and 4) are expected to extend indefinitely to the right, but numerical difficulties (too violent “explosions”) prevented us from continuing them further to larger values of  $r_h$ . They will intersect the (solid) curves for asymptotically flat solutions with  $n = 2, 3, \dots$  zeros of  $W$  and therefore yield additional asymptotically flat NAS black holes beside those found by Donets et al. [6], contradicting their uniqueness claim.

Finally there are the NAPRN solutions, which constitute a discrete set according to the number of available free parameters at  $r = 0$ . We found several such solutions with  $W'(0) = -1$  (compare Tab. 1). Only one of them has no maximum of  $r$  and was also found by Donets et al.

Table 1: Initial data for several NAPRN solutions with  $W'(0) = -1$ .

	$W_0$	$r_h$	$W_h$	# of zeros
1	0.9663634	0.7867834	1.54085646	0
2	0.93306559	1.889087974	0.29197873	0
3	0.9215847	0.8032373	-2.06670276	1
4	0.9150108	0.009594267	-0.8037193	1

## 5 Qualitative Discussion

We shall now give a qualitative picture of the solutions and try to explain our numerical results. Since the generic behaviour of the solutions is rather different in the cases with and without Higgs field, we shall treat the two cases separately. Let us first concentrate on the case without Higgs field. For simplicity we introduce the notation  $\bar{U} \equiv BW'$  and  $\bar{B} \equiv rB$  and use  $\sigma \equiv -\ln(r)$  as a radial coordinate. Observe that  $\bar{B} \approx -2m$  for small  $r$ . With these variables the field Eqs. (8) become (a dot denoting  $d/d\sigma$ )

$$\dot{W} = -r^2 \frac{\bar{U}}{\bar{B}}, \quad (31a)$$

$$\dot{\bar{U}} = -W \frac{W^2 - 1}{r} + 2r^2 \frac{\bar{U}^3}{\bar{B}^2}, \quad (31b)$$

$$\dot{\bar{B}} = r \left( \frac{(1 - W^2)^2}{r^2} - 1 \right) + 2r^2 \frac{\bar{U}^2}{\bar{B}}. \quad (31c)$$

Close to the horizon the first term in the equation for  $\bar{B}$  dominates (since  $\bar{U}$  vanishes at  $r = r_h$ ) and thus  $\bar{B}$  becomes negative. Provided  $W^2$  does not tend to 1, this term will, however, change sign as  $r$  decreases and  $\bar{B}$  will turn back to zero. Assuming further that  $\bar{U}$  does not tend to zero simultaneously, the second term in the equation for  $\bar{U}$  will grow very rapidly as  $\bar{B}$  approaches zero, leading to a rapid increase of  $\bar{U}$ . This in turn induces a rapid growth of  $\bar{B}$  (compare Fig. 1). Once the second terms in Eqs. (31b,c) dominate one gets  $(\bar{U}/\bar{B}) \approx 0$  and thus  $\bar{U}/\bar{B} = W'/r$  tends to a constant  $c$ . As long as  $(rc)^2$  is sizable  $\bar{U}$  and  $\bar{B}$  increase exponentially, giving rise to the phenomenon of mass inflation. Eventually this growth comes to a stop when  $(rc)^2$  has



become small enough. Then  $\bar{U}$  and  $\bar{B}$  stay constant until the first terms in Eqs. (31b,c) become sizable again. As before  $\bar{B}$  tends to zero inducing another “explosion” resp. cycle of mass inflation (compare Fig. 2).

In the discussion above we made two provisions – that  $W^2$  stays away from 1 and that  $\bar{U}$  does not tend to zero simultaneously with  $\bar{B}$ . If the first condition is violated, i.e.  $W^2 \rightarrow 1$  we get a NAS solution. If on the other hand  $\bar{U}$  and  $\bar{B}$  develop a common zero we get a NARN solution, i.e. a solution with a second horizon. Both these phenomena can occur after any finite number of cycles, giving rise to several NAS resp. NARN curves as in Fig. 4. Generically  $W$  changes very little during an inflationary cycle, with the exception of solutions that come very close to a second horizon, i.e. close to a NARN solution. In this case  $W$  may change by any amount, depending on how small  $\bar{U}$  becomes at the start of the explosion. By suitably fine-tuning the initial data at the horizon one can then obtain new NAS solutions with  $W \rightarrow \pm 1$  or a new NARN solution. In this way each NARN solution is the ‘parent’ of two NAS and one NARN solution. Fig. 4 shows two such generations: the NARN solutions labelled 2 have the NAS children 3 and 4 and the NARN child 5; the curves labelled 6 and 7 are the NAS children of 5 (see Fig. 5). Whenever the value of  $W$  at the second horizon of a NARN solution approaches  $\pm 1$  this NARN curve and its NAS children merge with the corresponding sibling NAS curve having one cycle less. This hierarchy of special solutions gives rise to a kind of chaotic structure in this region of ‘phase space’.

After this qualitative discussion we would like to present a simplified quantitative discussion of the solutions, following essentially one complete cycle. This will also provide us with a discrete map of the variables  $W, \bar{U}$  and  $\bar{B}$  from one plateau to the next. Let us denote their initial data at some plateau by  $W_0, \bar{U}_0$  and  $\bar{B}_0$ . Since the plateau is characterized by the (effective) vanishing of the second terms in Eqs. (31b,c) involving the factor  $r^2$  and the constancy of  $W$ , we can easily integrate them to

$$\bar{U} = \bar{U}_0 - \frac{W_0(W_0^2 - 1)}{r}, \quad \text{and} \quad \bar{B} = \bar{B}_0 + \frac{(W_0^2 - 1)^2}{r}, \quad (32)$$

ignoring the term  $-r$  in the  $\bar{B}$  equation. The beginning of the subsequent explosion is characterized by  $\bar{B} \approx 0$ , i.e.  $r \approx r_0 = -(W_0^2 - 1)^2 / \bar{B}_0$ . Depending on the value of  $W_0$  the value of  $\bar{U}$  at this point is essentially given by  $\bar{U}_0$  or  $-W_0(W_0^2 - 1)/r_0$ . Whatever it is, let us denote this value again by  $\bar{U}_0$ . For

the description of the solution through the explosion it is sufficient to solve the simplified system

$$\dot{W} = -r^2 \frac{\dot{\bar{U}}}{\bar{B}}, \quad \dot{\bar{U}} = 2r^2 \frac{\bar{U}^3}{\bar{B}^2}, \quad \dot{\bar{B}} = 2r^2 \frac{\bar{U}^2}{\bar{B}}, \quad (33)$$

implying  $\bar{U}/\bar{B} = c$  with some constant  $c$ . Plugging  $c$  back into Eqs. (33) we can integrate them to get

$$\bar{U} = \bar{U}_0 \exp\left(c^2(r_0^2 - r^2)\right), \quad (34a)$$

$$\bar{B} = \frac{\bar{U}_0}{c} \exp\left(c^2(r_0^2 - r^2)\right), \quad (34b)$$

$$W = W_0 + \frac{c}{2}(r^2 - r_0^2). \quad (34c)$$

We still have to determine  $c$  joining this solution to the one before the explosion. Equating the derivatives of  $\bar{B}$  at  $r = r_0$  using the expressions in Eqs. (32) and (34) we obtain  $c = \frac{(W_0^2 - 1)^2}{2\bar{U}_0 r_0^3}$ .

In order to obtain the values of  $\bar{W}_1, \bar{U}_1, \bar{B}_1$  after the explosion we may safely put  $r = 0$  in Eqs. (34) and obtain

$$\bar{U}_1 = \bar{U}_0 e^{(cr_0)^2}, \quad \bar{B}_1 = \frac{\bar{U}_0}{c} e^{(cr_0)^2}, \quad (35a)$$

$$W = W_0 - \frac{c}{2}r_0^2, \quad \text{with} \quad r_0 = -\frac{(W_0^2 - 1)^2}{\bar{B}_0}, \quad c = \frac{(W_0^2 - 1)^2}{2\bar{U}_0 r_0^3}. \quad (35b)$$

It is instructive to illustrate these relations on an example. We take the fundamental black hole solution with  $r_h = 1$  and  $W_h = 0.6322$  shown in Fig. 1. For the first explosion one finds the parameters  $r_0 \approx 2.7 \cdot 10^{-4}$  and  $c \approx 1.1 \cdot 10^5$  yielding  $cr_0 \approx 30$  and thus  $\bar{B}_1 \sim e^{900}$  and  $W_1 - W_0 \approx 4 \cdot 10^{-3}$ . The subsequent explosion will then take place at the fantastically small value  $r_0 \sim e^{-900} \approx 10^{-330}$ .

Since the change of  $W$  in one inflationary cycle has an extra factor  $r_0$  the function  $W$  stays practically constant. If we furthermore concentrate on cases, where the first term in Eq. (31b) can be neglected we may use the simplified system

$$\dot{W} = 0, \quad \dot{\bar{U}} = 2r^2 \frac{\bar{U}^3}{\bar{B}^2}, \quad \dot{\bar{B}} = \frac{(1 - W^2)^2}{r} + 2r^2 \frac{\bar{U}^2}{\bar{B}}, \quad (36)$$

also discussed by Donets et al. [6]. Introducing the variables  $x \equiv r\bar{U}/\bar{B} = W'$  and  $y \equiv -(1 - W^2)^2/r\bar{B}$  one obtains the autonomous system

$$\dot{W} = 0, \quad \dot{x} = (y - 1)x, \quad \dot{y} = y(y + 1 - 2x^2). \quad (37)$$

Since the first of these equations may be ignored, we can concentrate on the  $x, y$  part. As usual for 2-dimensional dynamical systems the global behaviour of the solutions can be analyzed determining its fixed points. Since the “large time” behaviour  $\sigma \rightarrow \infty$  corresponds to the limit  $r \rightarrow 0$  these fixed points are related to the singular solutions at  $r = 0$  discussed in chapter 3. There are essentially three different fixed points.

1. For  $y < 0$  there is the fixed point  $x = 0, y = -1$  giving the RN type singularity. Its eigenvalues are  $-1$  and  $-2$ , hence it acts as an attracting center for  $\sigma \rightarrow \infty$ .
2. Then there is the point  $x = y = 0$ , a saddle with eigenvalues  $\pm 1$ .
3. In addition there are the points  $x = \pm 1, y = 1$  with the eigenvalues  $1/2(1 \pm i\sqrt{15})$ , related to the pseudo-RN type singularity. This fixed point acts as a repulsive focal point, from which the trajectories spiral outwards. Since solutions of the approximate system given by the Eqs. (37) cannot cross the coordinate axes, solutions in the quadrants  $y > 0, x > 0$  resp.  $x < 0$  stay there performing larger and larger turns around the focal point coming closer and closer to the saddle point  $x = y = 0$  without ever meeting it. As observed by Donets et al. this nicely explains the cyclic inflationary behaviour of the solutions in the generic case.

Finally we come to the black holes with Higgs field. Apart from the generic solutions there are the special ones approaching  $r = 0$  with a singular behaviour described in chapter 3. On the other hand, the generic behaviour is much simpler than in the previously discussed situation without Higgs field. An easy way to understand this difference is to derive the analogue of the simplified system Eqs. (37). Introducing the additional variable  $z \equiv -\dot{H}$  and ignoring again irrelevant terms one finds

$$\dot{W} = 0, \quad \dot{H} = -z, \quad (38a)$$

$$\dot{x} = (y - 1)x, \quad \dot{z} = yz \quad (38b)$$

$$\dot{y} = y(y + 1 - 2x^2 - z^2). \quad (38c)$$

Leaving aside the decoupled equations for  $W$  and  $H$  one may study the fixed points of the  $(x, y, z)$  system. For  $z = 0$  one clearly finds the previous fixed points of the  $(x, y)$  system. However, for  $z \neq 0$  the focal point disappears and the only fixed point for  $y \geq 0$  is  $x = y = 0, z = z_0$  with some constant  $z_0$ . For  $z_0^2 < 1$  this point is a saddle with one unstable mode, whereas for  $z_0^2 > 1$  it is a stable attractor. The latter describes the simple inflationary behaviour described in chapter 4 and shown in the left part of Fig. 3. Solutions approaching a fixed point with  $z_0^2 < 1$  eventually run away from it again and ultimately tend to one with  $z_0^2 > 1$  as shown in the right part of Fig. 3. In both cases the Higgs field grows logarithmically as  $r \rightarrow 0$ .

Finally let us remark that all these solutions are singular at  $r = 0$ , since a regular origin requires  $B(0) = 1$ .

## 6 Summary

We study the behaviour of the static, spherically symmetric non-abelian black holes inside their event-horizon. We have chosen a Higgs field in the adjoint representation of  $SU(2)$ , but we expect similar results for Higgs fields in other representations, because for  $r \rightarrow 0$  the differences do not seem to be relevant.

In the generic case the solutions inside the horizon show a phenomenon known as “mass inflation” from perturbations of the Reissner-Nordström black holes at their Cauchy horizon. Whereas for the black holes with a Higgs field the mass function grows monotonously once the inflation has started those without Higgs field run through an infinite sequence of inflationary cycles, which take the form of ever more violent “explosions”. Besides the generic solutions there are exceptional ones with a Schwarzschild or Reissner-Nordström type singularity at the center of symmetry. These exceptional solutions accumulate in a way that may be interpreted as a kind of “chaotic” behaviour.

Since the typical length scale of these black holes is the Planck length (at least for values of the gauge coupling  $g^2/\hbar c$  of order one) one may question the physical relevance of these results of the classical theory. However, there are claims [10] that the phenomenon of mass inflation connected with the Reissner-Nordström black hole persists in the quantized theory. Definitely this subject requires further study.

Apart from that, our results provide a non-perturbative confirmation of

the mass inflation phenomenon observed for perturbations of the RN black hole. Furthermore we believe that our results are of some interest in view of the classical singularity theorems of Penrose and Hawking [1].

## 7 Acknowledgments

G.L. is grateful to Theory Group of the MPI für Physik for the invitation and kind hospitality during the visit in Nov. 1996, when this work was begun. He also wants to thank P.Hájíček for critical remarks and comments.

The work of G.L. was supported in part by the Tomalla Foundation and by the Swiss National Science Foundation.

## References

- [1] Hawking, S.W. and Ellis, G.F.R.: *The large scale structure of space-time*. Cambridge University Press, 1973.
- [2] Poisson, E. and Israel, W.: *Phys. Rev. D* **41** (1990) 1796.
- [3] Bonanno, A., Droz, S., Israel, W. and Morsink, S.M.: *Phys. Rev. D* **50** (1994) 7372.
- [4] Künzle, H.P., and Masood-ul-Alam, A.K.M.: *J. Math. Phys.* **31** (1990) 928;  
Volkov, M.S., and Gal'tsov, D.V.: *JETP Lett.* **50** (1989) 346;  
Bizon, P.: *Phys. Rev. Lett.* **64** (1990) 2844;  
Smoller, J.A., Wasserman, A.G., and Yau, S.T.: *Commun. Math. Phys.* **154** (1993) 377.
- [5] Breitenlohner, P., Forgács, P., and Maison, D.: *Commun. Math. Phys.* **163** (1994) 141.
- [6] Donets, E.E., Gal'tsov, D.V. and Zotov, M.Yu.: *Internal Structure of Einstein-Yang-Mills Black Holes*.  
gr-qc/9612067.
- [7] Breitenlohner, P., Forgács, P., and Maison, D.: *Nucl. Phys. B* **442** (1995) 126.

- [8] Breitenlohner, P., Forgács, P., and Maison, D.: *Nucl. Phys.* **B 383** (1992) 357.
- [9] Coddington, E.A., and Levinson, N.: *Theory of Ordinary Differential Equations*. New York: McGraw-Hill, 1955.
- [10] Oda, I.: *Mass Inflation in Quantum Gravity*. gr-qc/9701058.